

**Errors of Interannual Variability and Multi-Decadal Trend in Dynamical Regional
Climate Downscaling and Their Corrections**

Masao Kanamitsu, Kei Yoshimura,

Scripps Institution of Oceanography, University of California, San Diego

and

Yoo-Bin Yhang and Song-You Hong

Yonsei University, Seoul, Korea

February 4, 2009

To be submitted to Monthly Weather Review

Corresponding author: Dr. Masao Kanamitsu, Mail Code 0224; CRD/SIO/UCSD; 9500
Gilman Drive; La Jolla, CA 92093-0224
E-mail: mkanamitsu@ucsd.edu

Abstract

The interannual variability of dynamically downscaled analysis and its large scale error relative to global coarse resolution analysis is examined in this paper. It is shown that the large scale regional model error significantly contaminates the interannual variability of the seasonal mean. The error occupies significant part of the interannual variability, particularly during summer season. Accordingly, the leading modes of Empirical Orthogonal Functions (EOFs) of 500 hPa height in the region are very different from those of the global analysis.

The Scale Selective Bias Correction (SSBC) method by Kanamaru and Kanamitsu (2003) is refined to further reduce the large scale error within the observational error. Application of this method in dynamical downscaling reduced the error of the interannual variability of analysis fields (namely, height, temperature and winds), and made the EOFs of seasonal mean 500 hPa height agree well with that of the global analysis.

The application of the SSBC made modest impact on model derived fields, such as precipitation and near surface air temperature. The improvements in these fields are not as dramatic as in the analysis fields,

but the increase in simulation skill is found to be apparent.

The paper also discusses the implication of the method to general downscaling problems, including the downscaling of global change simulations.

1. Introduction

The dynamical downscaling has been used extensively in making small-scale regional scale analyses, forecasts and simulations for the past two decades or more. In recent years, due to the public demands of predicting and projecting impact of global change to local community and society, focus was placed on the dynamical downscaling of climate time scale and global change simulations. In fact, in the IPCC assessment, the downscaling has been one of the major topics from the beginning, and the demand is growing even further.

The dynamical downscaling on the climate time scale, as in the downscaling of global change simulations, has been examined in terms of its ability to simulate interannual variability. Alexandru et al (2007) discussed that the internal variability in regional downscaling results from two sources: (1) variability forced by the lateral boundary and by the surface characteristics, which is considered to be reproducible and (2) the internal variability simulated by regional model, which is not reproducible. The latter can be separated from former by utilizing ensemble integration methods with perturbed initial conditions under the same lateral boundary forcing. Giorgi and Bi (2000), Christensen et al (2001), Rinke et al (2004) and Alexandru et al (2007) examined the internal variability in detail and concluded that it strongly depends on

model configuration (domain size and resolution), synoptic situation, variables and location.

In this paper, we discuss that the internal variability can further be separated into two components: (1) physically unpredictable part and (2) time varying model error. Apparently, it is not possible to separate the internal variability into these two components unless the truth is known. In the cases of downscaling of atmospheric analyses, the truth is known for the *analysis fields* whose scales are greater than a predetermined size for which the analysis is considered to be accurate. When estimated from the spatial density of the available observations, this scale is of the order of 500 to 1000km in most of the operationally produced global objective analysis,. Thus, in the case of the downscaling of global analysis, it is possible to extract the time varying error component of the internal variability for the scale greater than 500-1000km. Even more, since truth is known, it may be possible to develop a method to reduce or even eliminate the error.

If we extend this notion further, in the cases of downscaling of global model forecasts or simulations for which truth is not known, it is still reasonable to assume that the scale greater than 500-1000km is accurate in the simulation, or at least more accurate than the prediction with regional models, and thus, we can extract the error part

of the internal variability. It is dynamically and physically logical to assume that the global model forecast/simulation of planetary scale is more accurate than the regional ones since simulation without artificial lateral boundary will be more dynamically and thermodynamically natural, consistent and “correct”. We have to remind that this notion does not hold for regional initial value problems (short range forecasts), since effect of lateral boundary can be overwhelmed by that of the initial condition. In this sense, the regional short range forecast, which is more of an initial value problem, is fundamentally different from a continuous downscaling used frequently in the dynamical downscaling of climate time scale. Thus, in the cases of the continuous downscaling of model simulations, we may again detect the “large scale errors” and correct them during the integration process.

The application of the correction of “large scale errors” during the regional model integration may be re-interpreted as the following definition of the dynamical downscaling: *“The dynamical downscaling is a diagnostic tool to attain regional scale detail under the given large scale forcing.”* The important point here is that the dynamical downscaling is a “*diagnostic tool*” and not a prognostic one. This definition is also consistent with the assumption of one-way nesting made in dynamical downscaling, where regional model large scale simulation is not allowed to alter the

global coarse resolution forcing. This definition is frequently forgotten by some people engaged in dynamical downscaling, who believe that even the large scale can be “improved” by the high resolution regional model. This is definitely not true for long continuous dynamical downscaling.

In this paper, we will demonstrate that the “error” part of the internal variability is very large and significantly contaminates the interannual variability of the large scale part of the downscaled field. By deduction from these results, we may also conclude that the dynamical downscaling of global change simulations will also be contaminated by the regional model error to a similar degree. We also try to show that the contamination of interannual variability also affects the long term linear trend.

The above discussions imply that it is important to introduce some sort of “correction” to prevent the interannual variability from contaminating the downscaled analysis. We show that the Scale Dependent Bias Correction (SSBC) method proposed by Kanamaru and Kanamitsu (2005) is a powerful method to perform this “error correction”. With additional improvements to the method, it is shown that the error can be reduced to a range of observational error.

In this paper, we will first review our correction method developed by Kanamaru and Kanamitsu (2006), and its improvement in Section 2. We describe

experiment design in Section 3. Section 4 discusses the effect of model error on interannual variability. Section 5 examines the interannual variability of derived fields, namely near surface temperature and precipitation. The conclusion is given in Section 6.

2. Review and Refinement of the Scale Selective Bias Correction (SSBC)

Kanamaru and Kanamitsu (2005) developed a method to correct large scale regional error based on the idea proposed by Kida et al. (1991) and von Storch et al (2000). The brief outline of the method is described below:

A term is introduced to the zonal and meridional momentum equations to “nudge” the difference between the background global model/analysis field and regional forecast field (hereafter named perturbation) to zero for a scale greater than a critical length in two dimensional wave space.

$$F_t^{new}(m,n) - F_{t-\Delta}(m,n) = \left(\frac{1}{1+\alpha} \right) \cdot (F_t^{old}(m,n) - F_{t-\Delta}(m,n)) \text{ for } m,n < m_c, n_c \quad (1)$$

where F_t is the perturbation, expressed in spectral coefficient form, with two dimensional wavenumbers m and n (in the x and y directions, respectively) at time t .

$F_{t-\Delta}$ is a spectral coefficient one time step earlier. The superscripts “old” and “new” indicate the values before and after the damping. A damping coefficient α has a value of 0.9 which is determined from multiple trial and error integrations. The equation (1)

is derived from implicit time scheme to avoid numerical instability. Note that in this formulation, the dumping is applied to the time tendency of perturbations. The critical scale is set to physical scale of 1000km, and the critical wavenumber m_c and n_c vary with domain size and model resolution. For temperature and moisture, the area average perturbation is set to zero every time step, but no dumping is applied to wave coefficients. In addition, surface pressure is corrected to account for the difference in surface altitude between the coarse resolution global model/analysis and regional model. Using these methods, Kanamaru and Kanamitsu (2005) demonstrated that the large scale does not deviate significantly from global forcing, the simulation becomes insensitive to the choice of domain size and the skill of precipitation simulation improves.

During the course of the validation of the long period downscaling of reanalysis (CaRD10, Kanamitsu and Kanamaru, 2007; Kanamaru and Kanamitsu, 2007), it is found that even with SSBC, the large scale error within the domain can occasionally grows to a significant amplitude. We decided to perform further experiments to improve the SSBC, by more carefully selecting nudging variables, nudging method and the magnitude of nudging. We also discovered that the lateral boundary nudging zone width and nudging strength is closely related to the amplitude

of the large scale model error which is controlled by the SSBC. The lateral boundary zones used in the original SSBC are rather broad, 23 % of zonal and meridional lengths of the domain (11.5 % for each side) which reduces the region of useable domain by nearly 40%. Even a small reduction of the nudging zones is considered to be beneficial.

After many trial runs, we found that the following five modifications decrease the errors, improve the model performance and reduce the lateral boundary zone:

(1) The nudging is applied to perturbation rather than its tendency with the same nudging coefficient. This places slightly stronger constraints, and maintain the error small, i.e.,

$$F_t^{new}(m,n) = \left(\frac{1}{1+\alpha} \right) F_t^{old}(m,n) \quad \text{for } m,n < m_c, n_c \quad (2)$$

(2) The nudging is applied only to the rotational part of wind. This has the effect of minimizing spurious surface pressure oscillations, and tends to better maintain the large scale balance between mass and motion fields.

(3) The area average correction of moisture is removed and only the area averaged temperature is corrected. The removal of moisture correction minimizes the significant bias in the simulation of precipitation especially in lower latitudes caused by the inconsistencies of physical packages between the forcing and the

RSM.

- (4) By the stronger spectral nudging over the domain combined with other changes, it became possible to narrow the lateral boundary zones to 5 % (from original 23%) of zonal and meridional width of the domain (2.5 % each side) and also to reduce the nudging coefficients to a minimum to just keep the integrations stable.
- (5) The diabatic processes are removed from the lateral boundary zone, although its impact was minimal.

The comparison of the performance of this refined SSBC and original scheme over United States and over Amazon are described in Appendix.

3. Model and experimental setup

3.1 Model

The spectral representation of the RSM is a two-dimensional cosine series for perturbations of pressure, divergence, temperature, and mixing ratio, and a sine series for vorticity. The physical processes in the RSM follow the package of Hong and Leetmaa (1999), except for the revised vertical diffusion scheme of Hong et al. (2006). Long- and short-wave radiation interact with clouds, non-local treatment for the planetary boundary layer process, deep and shallow convection, large-scale condensation, gravity wave drag, hydrology model, and vertical and horizontal diffusion

are considered. Land surface and soil physics use the two-layer model of Mahrt and Pan (1984), which includes soil thermodynamics and hydrology as diffusion processes. Precipitation is produced by both large-scale condensation and the convective parameterization schemes. The large-scale precipitation algorithm tests for super-saturation in the predicted specific humidity. Latent heat is released when the specific humidity exceeds the saturation and the temperatures and humidity are adjusted to bring the humidity to saturation. The scheme does not include a prognostic cloud; however, the evaporation of rain in unsaturated layers below the level of condensation is taken into account.

The major differences between this model and the model used in NCEP/DOE analysis are the short and long wave radiation and detail in the convective parameterization. As one might expect, the detail of the physical processes of the model is not important in this study.

3.2 Experimental design

For the study of interannual variability and trend, we chose the model domain covering the East Asia Monsoon region centered at 35° N, 127.5° E, from the eastern flank of the Tibetan Plateau in the west to the northwestern Pacific Ocean in the east (Fig. 1). The choice of the area is somewhat arbitrary, but the area believed to represent typical

mid-latitude circulations. The model grids consist of 109 (west-east) by 86 (north-south) grid points at approximately 60 km horizontal separation at 60N, and 28 sigma layers in the vertical. The simulations were performed for 25 summers (June 1 to August 31) and winters (December 1 to end of February the following year) from 1979 to 2003. Initial conditions and large-scale forcing are obtained from the 6 hourly NCEP-DOE reanalysis (R-2) data (Kanamitsu et al., 2002). Observed sea surface temperature (SST) is updated daily from the optimal interpolation SST (OISST) weekly dataset (Reynolds and Smith, 1994). One may argue that the spin-up is necessary to adjust the soil initial conditions, as done in the previous studies (e.g., Gochis et al. 2002). However, the preliminary results using the RSM, also as described in Kang and Hong (2008), showed that such a spin up is unnecessary when the RSM is forced by the reanalysis data. This is because the effect of atmospheric forcing is much stronger than the land surface forcing, particularly when SSBC is applied. It may also be due to the fact that the RSM employs the soil physics package (Mahrt and Pan 1984) and the soil and vegetation types similar to those used in the R-2 data assimilation system.

4. Interannual variability of geopotential height and wind

In this section, we analyze the interannual variability of the seasonal mean field simulated by the RSM. We compare the three runs; (1) without spectral nudging

(NOSSBC), (2) original spectral nudging (SSBC) and (3) refined nudging (NEWSSBC) for summer and winter cases (for winter, experiments (2) is not performed). Since low frequency variability tends to have large spatial scale, these comparisons are equivalent to examining large scale internal model variability and large scale model error in the regional domain. The small scale features produced by high resolution regional model will also be affected by the simulated large scale, since the error in large scale affects the location and intensity of the regional scale “system”. This will be studied in the Section 5.

4.1 Mean difference and interannual variance

In Figure 1, we show the 1979-2005 R-2 climatology and errors of three model simulations. Even for the long time mean, the error in the height field without SSBC (NOSSBC) is of the order of 10 to 15 meters, not negligibly small. This error is only slightly smaller (about 15 meters) than the interannual variability shown in Figure 5. The error has very broad scale of wavenumber one in east-west with its wavelength of about 2000km. The pattern of error indicates that the climatological trough located over the coast of Russia-China-Korea is shifted towards west and becoming sharper in summer, but it may be a reflection of an excitation of some sort of erroneous computational mode in the limited domain. The Fig. 1 also shows that the original

SSBC is working moderately to reduce the error by about 5 meters, while the refined SSBC is working excellently to remove the error within 5 meters. Similar results are found for 850 hPa winds (Figure 2) and 200 hPa wind speed (not shown), all showing that the error of NOSSBC is large and refined SSBC reduced it significantly. Particularly at 850hPa, the error pattern over Pacific indicates northwards shift of the subtropical ridge, crucial for the summertime simulation over Japan, is nearly eliminated in the NEWSSBC run. This northward shift is a very common model error found in many simulations (e.g., Kusunoki et al., 2006). During winter, the systematic error is larger (Figure 3). The 500 hPa height error for NOSSBC is greater than 15m, has much larger scale, indicating somewhat deeper climatological trough without a shift in location. The NEWSSBC again reduces the error to less than 5 meters.

In order to examine how the error evolves with year, Figure 4 displays the year-to-year variability of Root Mean Square (RMS) error of 500 hPa height over the domain for summer (upper panel) and winter (lower panel). The RMS difference of R-2 analysis from long time mean is also plotted as a measure of the interannual variability. It is clearly seen that without any error correction, the error is large and varies significantly from year to year. The error can become larger than the

interannual variability in 11 summers and 4 winters in 25 years. The error correction is working nicely as expected and the new version corrects the error within 2-3 meters, with very small interannual variability both in summer and winter.

The geographical distribution of interannual variability of 500 hPa height in summer, shown in Figure 5 (first row), clearly demonstrates where the error dominates. The variability is nearly the same between R-2 and the new version of SSBC, while the run without SSBC significantly increase the interannual variability in the area near the center of the domain, where the variability is more than 30% larger than R-2. During the winter (Fig. 5, second row), the patterns of interannual variability between R2 and NOSSBA are not far apart, although without SSBC, the variability is enhanced by 10-20% in the middle of the region.

4.2 Empirical Orthogonal Function

The EOFs of summertime seasonal mean 500 hPa heights are compared in Figure 6 for the first three modes. The first mode (top row) in no SSBC (second column) has quite different pattern than the others. Apparently, the regional model error produces its own interannual variability and contaminates the low frequency variability in the global forcing. Mode 2 (2nd row) for no SSBC (second column) is also very different from R2 and others, while all the patterns look very similar for Mode

3 (3rd row). The SSBC corrections are working nicely as before. The original SSBC corrects most of the error in EOFs, but the refined SSBC makes the EOF patterns much closer to those of the R-2. The EOF of the difference between R2 and each experiment is shown in Figure 8. There is a distinct patterns in NOSSBC and original SSBC, but not in NEWSBC. The model error tends to grow in an organized manner, varies from year to year in response to the change in large scale forcing. This result suggests that the interannual variability in regional downscaling by Giorgi and Bi (2000), Christensen et al (2001), Rinke et al (2004) and Alexandru et al (2007), are partly the artifact of the interannual variability of regional model error, which varies significantly from year to year.

During winter, interannual variances are again different if no SSBC is applied (Figure 5, second row). However, the first 3 mode of the EOF (Figure 8) are much more alike between all the experiments. This similarity is explained by the fact that the interannual variability in winter is generally larger than the variability of the model error.

4.3 Linear trend

The linear trend of 500 hPa height is compared in Figure 9. We see again that the run without SSBC is very different from R-2 in magnitude and pattern, and the

correction is working well. For example, over northern Japan in summer, the sign of the trend changes from negative in R-2 to positive in NOSSBC. During the winter, the pattern of the trend is not too different between the three experiments, but the magnitude was significantly underestimated in NOSSBC run. The difference between R-2 and NEWSSBC is greater than that in summer.

In summary, the regional model has large scale error that varies from year to year. This error contaminates interannual variability. The magnitude of the error is large enough to modify the leading EOFs and even the sign of the linear trend, particularly in summer season. The large scale error correction scheme, if properly incorporated, is able to significantly reduce these errors.

5. Impact on precipitation and surface temperature

In the previous section, interannual variability of large scale field error, namely 500 hPa height, 850 hPa wind and 200 hPa winds are examined. Since these parameters are closely connected with the variables the SSBC is applied in the basic set of equations, it is not surprising if the SSBC reduces the error.

The more important question to be examined here is the error in the derived fields, such as precipitation, near surface temperature, surface and radiation fluxes, soil moisture, and many other parameters derived from model integrations. As we might

question, even if the large scale forcing is correct, these variables may suffer from error due to deficiencies in model physical parameterizations and as a result, we may not see the impact of SSBC in those parameters as clearly as in the height and wind fields.

5.1 Mean difference and interannual variance

As a start, let us examine the large scale pattern of the precipitation. Figure 10 compares precipitation between the observation (CMAP) and the three experiments during summer and winter (two experiments for winter). In summer, there is a tendency that the model produced precipitations are more similar to each other than to the observation, as seen in the wide spread precipitation over the continent. The CMAP is a large scale precipitation analysis and we should not expect small scale features to agree with model, but the difference in large scale pattern is clear. The small scale precipitation in the main island of Japan, Korea and the coastal Russia are the features probably not obtainable from CMAP. Among the downscaled analyses, SSBC has greater overestimation than others, making it stands out. This is a result of area mean moisture correction, which is removed in NEWSSBC (and not in NOSSBC to start with). During the winter time (Fig. 10, second row), model produced large scale precipitation patterns are very similar to each other and to observation, except the small scale precipitation maximum along the Sea of Japan coast of main Japanese

islands, which cannot be resolved by CMAP. The overestimation of precipitation is apparent in NOSSBC, but not as much during the winter. These comparisons indicate that the large scale precipitation pattern is not critically affected by the large scale error in the atmospheric circulation, at least for this region with the current choice of the domain. This result implies that the precipitation simulation is more strongly affected by its parameterization and not by the errors in the large scale forcing.

When it comes to the interannual variability, we start observing significant differences among the model simulations. Figure 11 is the EOF of precipitation during summer. For Mode 1, the patterns of model simulations are not so close to the observed pattern, but NEWSSBC and SSBC resemble more with CMAP than that of NOSSBC. Somewhat disorganized EOF patterns in model simulations indicate that the model response is weaker to interannual variability in large scale forcing, but the correction of large scale certainly helps in improving the simulation of precipitation variability. For the second mode, all the model simulations are very different from CMAP, indicating more problems with the model simulation. Another interpretation may be that the precipitation is not directly connected with the interannual variability of the large scale circulation, but this is very unlikely. During winter (Figure 12), the story is quite similar to that in summer, and NEWSSBC is again slightly better in mode

1 and mode 2. There is a systematic difference in the location of maxima in Mode 1 for NEWSSBC, which is shifted southward by 2-3 degrees latitude. The similarity of mode 2 between R-2 and NEWSSBC is not so strong, and the pattern is disorganized in NEWSSBC. Once again, the interannual variability of forcing is not directly reflected in the model simulation. Note that the EOFs of NOSSBC agrees much less than those of the NEWSSBC, indicating modest impact of SSBC on precipitation.

5.2 Linear trend

Figure 13 compares the linear trend of precipitation during 1979-2005. The model simulations present much smaller scale patterns with trend of opposite signs. However, large scale patterns, such as the positive trend in southwest China, negative trend over the central northern part of the domain and positive trend over northeast corner of the domain all agree with CMAP trend in summer. The narrow band of negative trend oriented from northeast to southwest located right over Japan in NOSSBC seems to have different orientation of east-north-east to west-north-west in SSBC, but more disorganized in NEWSSBC. During the winter time, even the large scale patterns are not so similar to each other, with much enhanced trend in model simulations. Apparently, linear trend of precipitation is very sensitive to the small change in large scale forcing field.

Figure 14 compares the linear trend of near surface air temperature. In summer, all the model simulations agree well with R2, while in winter, NEWSSBC seems to agree better with observed trend. The near surface temperature trend seems to be more insensitive to the change in large scale forcing during summer, but is more sensitive in winter. This may be explained from the fact that the near surface temperature is more strongly controlled by the land surface conditions (soil moisture, and surface albedo) in summer but is influenced more strongly by large scale circulation in winter. Therefore, the impact of SSBC can be more apparent during the winter season.

5.3 Validation of precipitation against station observation

Since CMAP represents large scale features of the observed precipitation, it may not be appropriate to validate simulated small scale model precipitation. We tried to compare the simulated precipitations directly with station observations over Japan, where meso-scale hourly precipitation observations are readily available. The observation network is named AMeDAS (Automatic Meteorological Data Acquisition System), distributed throughout Japan with average distance of stations of 20-30km. Figure 15 compares summer and winter-time seasonal correlation of seasonal mean precipitation against AMeDAS observations averaged over several sub-regions over

Japan (Fig. 15a). During JJA (Fig. 15b), correlation is about 0.6-0.8 for all areas with NEWSBC, much better than other experiments, clearly demonstrating the effectiveness of the SSBC in simulating interannual variability of seasonal mean precipitation. The improvement is not so large during winter (Fig. 15c), but some northern areas (N-Hokkaido and S-Hokkaido) show better agreement. This validation against observation again suggests that the correction to the large scale forcing is important in properly simulating interannual variability of precipitation in meso-scale. The effect is greater in summer than in winter.

6. Conclusions and discussions

This paper examines the role of large scale error of regional model and its effect on interannual variability in dynamical downscaling. It is demonstrated that conventional dynamical downscaling methods without any large scale error corrections suffer from large scale regional model error that contaminates interannual variability and linear trend of downscaled fields. The error also contaminates low frequency variability and trend of derived fields, such as precipitation. The effect of model error on the variability is greater in summer time, as the magnitude of the error is comparable to the interannual variability of seasonal mean.

These results are obtained from dynamical downscaling of NCEP/DOE

reanalysis during 1979-2005 over far eastern Asia, using Scripps Institution of Oceanography Regional Spectral Model at 50km resolution. The model was run during summer (JJA) and winter (DJF) period for 25 years.

In order to improve downscaling, the original version of the Scale Selective Bias Correction (SSBC, Kanamaru and Kanamitsu, 2003) is refined to further reduce the large scale model error. This was accomplished by replacing the nudging of tendency in the original version to the nudging of field itself, nudging the rotational part of the wind only, removing the area average moisture correction and reducing the lateral boundary nudging zone width and strength. The refined SSBC reduced the interannual variability of seasonal mean 500 hPa height to within 5 meter and nearly eliminated the error in interannual variability.

The impact of correcting large scale error in simulating precipitation and near surface temperature was found to be modest. This somewhat reduced impact is due to the inaccuracies in the precipitation process in the model, which is not able to faithfully reproduce observed precipitation given large scale forcing, particularly its interannual variability. However, the modest impact implies that even with somewhat deficient parameterization, the correction to large scale forcing works positively to reduce error and improve dynamical downscaling.

The large scale model error examined in this paper would be a strong function of the choice of the model domain, its location, model resolution and physics of the model. It is very likely that the error increases as the domain size increase (consider the case when the domain is expended to hemisphere, for example). The error might grow larger in the area of complex topographic areas, and in the tropics where the parameterized physics controls the accuracy of the simulations. In this regard, it seems important to apply SSBC to all the cases, which have a potential of improving the simulations of mean as well as interannual variability.

Regarding the use of SSBC in the downscaling of GCM simulations, for which truth is not known, our recommendation is to utilize it fully. Although it is not possible to obtain large scale regional model error, it is more logical to faithfully apply the large scale forcing simulated by the global model without altering it by the regional model. It should be emphasized again that the dynamical downscaling is a diagnostic tool to obtain small scale features forced by given large scale forcing, thus the large scale forcing should not be modified during the downscaling procedure.

The large scale errors in regional model are caused by multiple reasons. Some of the critical ones are the mathematically ill-posed lateral boundary condition, error or inconsistency between regional model solution and global model forcing due to

difference in model numerics, physics and resolution. Some of those can be improved by developing new numerical techniques, new physical packages and others, but it is impossible to entirely eliminate the model error and also will take significant amount of time and effort. In this regard, the SSBC is a practical alternative to eliminating/reducing the errors. One concern of using SSBC is that the addition of nudging term may distort some of the physical and dynamical processes in the model, making some physical processes unphysical. So far, we think that such problem is not occurring in our case since the model error is of large scale and significantly smaller than other leading terms in the prediction equations.

Appendix

This appendix briefly shows the performance of the refined SSBC scheme. We performed three experiments; 1) the original SSBC, 2) narrow lateral boundary zone without SSBC (LBN), and 3) a new improved SSBC (SN) with narrow lateral boundary zone. In order to examine more general performance of the change in the SSBC, the integrations were performed over two regions, one over North American domain (10-50N, 65-135W), and the other over Tropical South American domain (20S-15N, 30-90W). The integration period is arbitrarily chosen from March 1st to 10th, 1985. The root mean square differences (RMS) from the forcing fields, NCEP/DOE Reanalysis 2, are used as a measure of the large scale error. We exclude details of the model descriptions used in this study, except that they are very similar to the ones described in Section 3.1.

Table 1 summarizes the results of those experiments. The refined SSBC worked best over both North America and South America in reducing 500 hPa height RMS error, although less in the tropics. The improvement in surface pressure is also apparent. The SSBC generally improves fit of mass field (except small degradation of 500 hPa height in North America). The overestimation of precipitation in original SSBC was corrected both in NO-SSBC and refined SSBC by the removal of the area average

correction of moisture. These experiments suggest that the refined SSBC considerably improves upon the original SSBC.

Acknowledgements

This work was funded by NOAA (NA17RJ1231) and the California Energy Commission Public Interest Energy Research (PIER) program, which supports the California Climate Change Center (Award Number MGC-04-04) and. The views expressed herein are those of the authors and do not necessarily reflect the views of NOAA. The assistance of Ms. D. Boomer in refining the writing is appreciated.

Figure Captions

Figure 1. 1972-2005 summer (JJA) climatology of 500 hPa geopotential height. R-2 stands for NECP/DOE reanalysis, error of runs without SSBC (NOSSBC-R2), with original SSBC (SSBC-R2) and NEWSSBC (NEWSSBC-R2) are shown in the second row. Unit in meter.

Figure 2. Same as Figure 1 but for 850 hPa winds. Unit in meter/sec. Blue shading for wind speed overestimate more than 5m/s, brown for underestimate of more than 5m/s.

Figure 3. Same as Figure 1 but 500 hPa height during winter (DJF). Unit in meter/sec. Original SSBC experiment is not performed.

Figure 4. Interannual variability of 500 hPa height root mean square error over the domain for summer (upper panel) and winter (lower panel). NOSSBC stands for without SSBC, SSBC for original SSBC and NEWSSBC for refined SSBC. Unit in meter. Orange line indicates interannual variance of height from R-2 observation.

Figure 5. Geographical distribution of interannual variability of seasonal mean 500 hPa height for summer (first row) and Winter (second row). Unit in meter. Note the different color coding between summer and winter.

Figure 6. Leading three modes of summer time 500 hPa geopotential height EOF for analysis (R2) and experiments during summer. The percent variance is indicated by percent in each panel.

Figure 7. First three modes of the EOF of 500hPa height model error. Percent variances are also indicated in each panel.

Figure 8. Same as Figure 6, but during winter.

Figure 9. 1972-2005 linear trend of 500 hPa height for summer (upper panels) and winter (lower panels). Unit in meter/10 years.

Figure 10. 1978-2005 climatology of precipitation for summer (upper panes) and winter (lower panels). Unit in mm/month.

Figure 11. First two leading EOF of seasonal mean precipitation during summer from observation (R-2) and experiments.

Figure 12. Same as Figure 11 but for winter.

Figure 13. 1978-2005 linear trend of precipitation during summer (upper panels) and winter (lower panels). Unit in mm/10 years.

Figure 14. 1978-2005 linear trend of near surface temperature during summer (upper panels) and in winter (lower panels). Unit in mm/10 years.

Figure 15. Temporal correlation of precipitation at AMeDAS stations average over

sub-domains in summer (b) and winter (c). The domains are color coded (a) by orange (N-Hokkaido), green (S- Hokkaido), magenta (Tohoku), yellow (Kantou), red (Chubu), blue (Kinki), brown (Shikoku), purple (Kyushu) and light green (Okinawa).

Table 1: Performance of the regional model integrations with different spectral nudging methods and boundary condition treatments.

	500 hPa height	sea level pressure	Total
	RMS (m)	RMS (Pa)	precipitation (mm/day)
North America			
SSBC	23.3	264.0	1.99
NO-SSBC	21.1	300.8	1.59
Revised SSBC	13.8	214.0	1.52
Tropical South America			
SSBC	11.4	158.0	8.30
NO-SSBC	28.7	377.7	4.51
Revised SSBC	11.3	151.8	4.67

JJA 25-year 500-hPa height climatology and error (m)

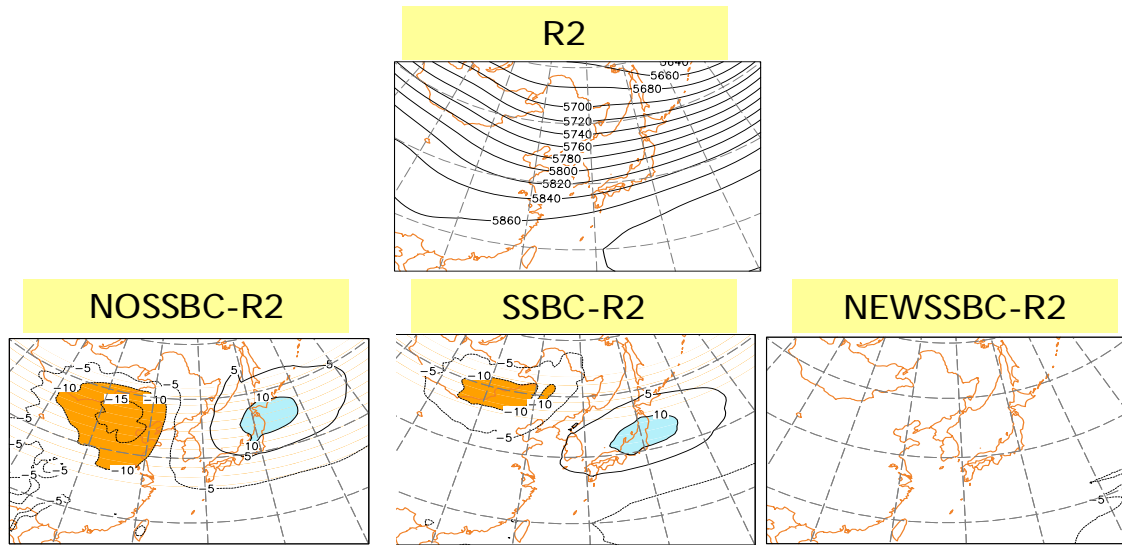


Figure 1. 1972-2005 summer (JJA) climatology of 500 hPa geopotential height. R-2 stands for NECP/DOE reanalysis, error of runs without SSBC (NOSSBC-R2), with original SSBC (SSBC-R2) and NEWSSBC (NEWSSBC-R2) are shown in the second row. Unit in meter.

JJA 25-year 850-hPa wind climatology and error (m)

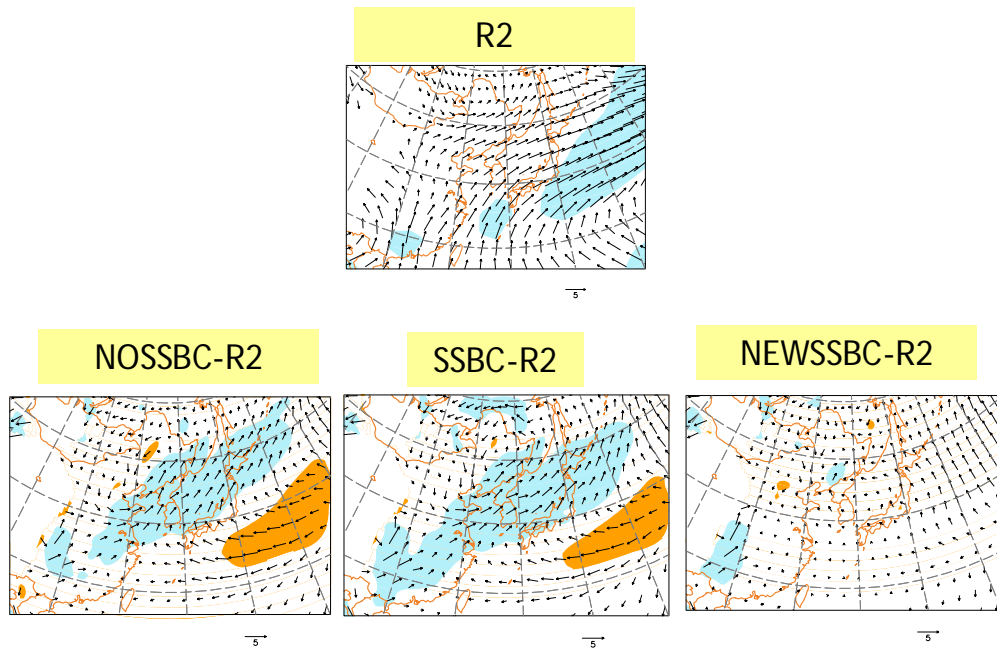


Figure 2 Same as Figure 1 but for 850 hPa winds. Unit in meter/sec. Blue shading for wind speed overestimate more than 5m/s, brown for underestimate of more than 5m/s.

DJF 25-year 500-hPa height climatology and error (m)

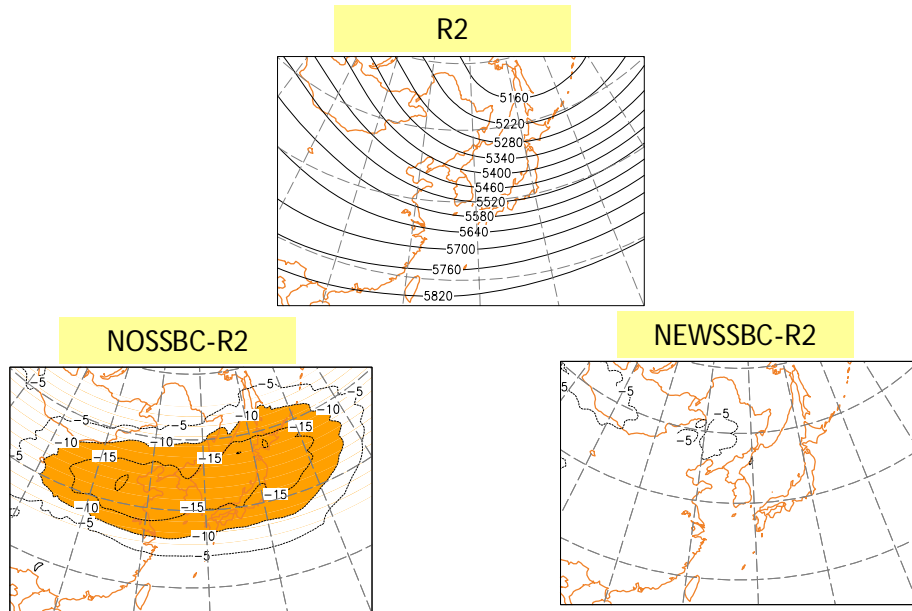


Figure 3. Same as Figure 1 but 500 hPa height during winter (DJF). Unit in meter/sec. Original SSBC experiment is not performed.

Interannual variation of 500-hPa height RMSE

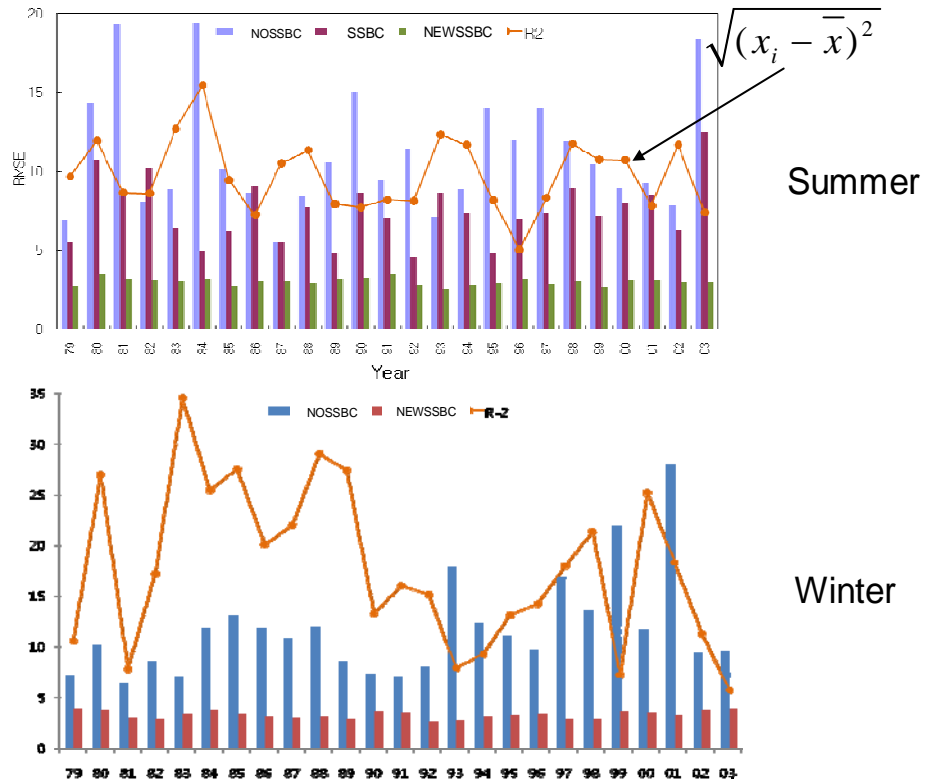


Figure 4. Interannual variability of 500 hPa height root mean square error over the domain for summer (upper panel) and winter (lower panel). NOSSBC stands for without SSBC, SSBC for original SSBC and NEWSSBC for refined SSBC. Unit in meter. Orange line indicates interannual variance of height from R-2 observation.

interannual variability of 500-hPa height

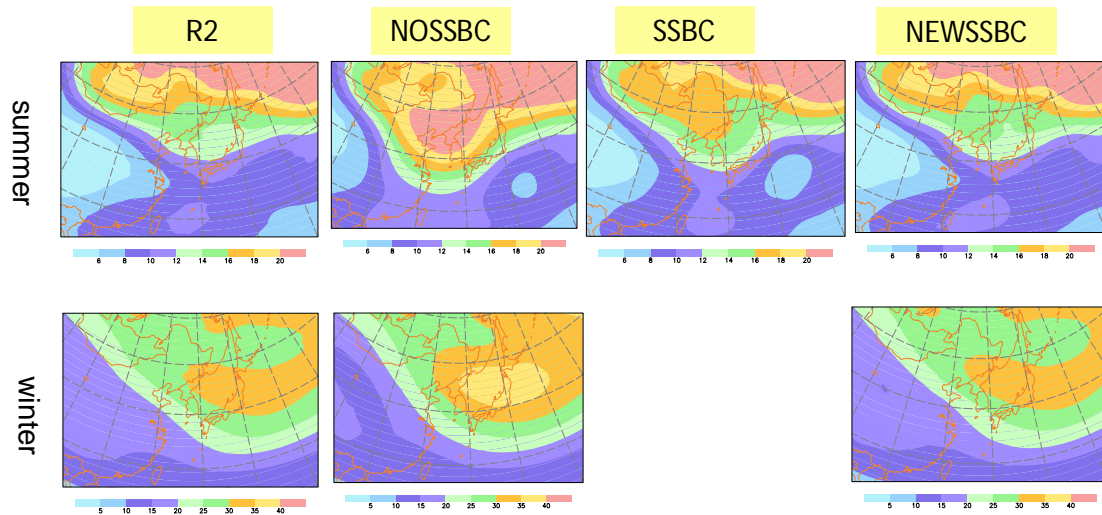


Figure 5. Geographical distribution of interannual variability of seasonal mean 500 hPa height for summer (first row) and Winter (second row). Unit in meter. Note the different color coding between summer and winter.

500-HGT EOF JJA

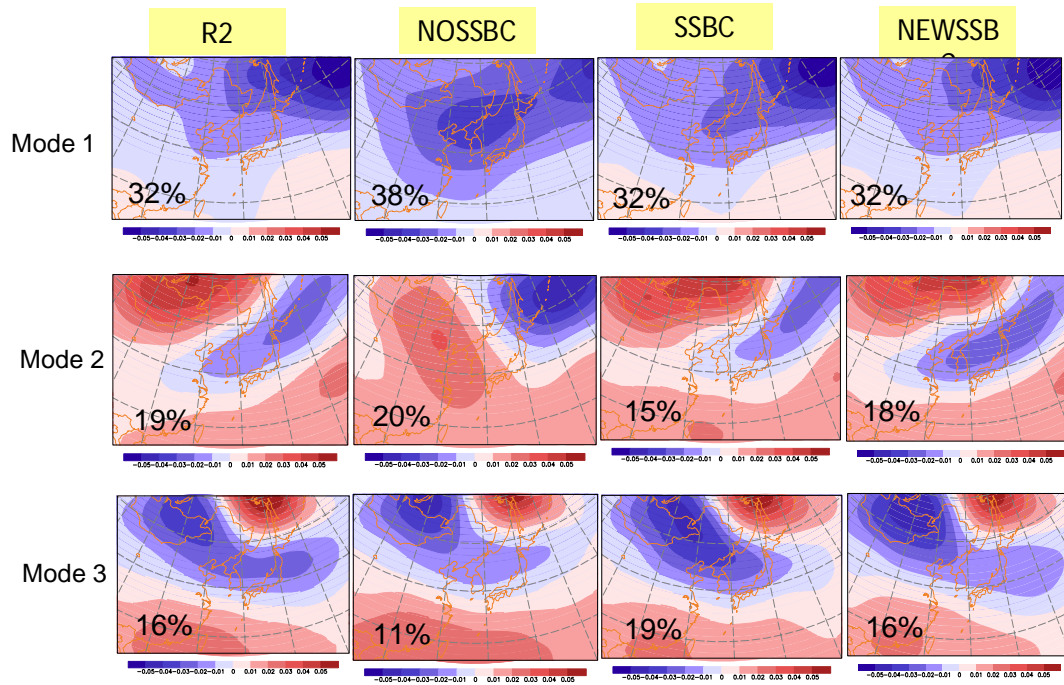


Figure 6. Leading three modes of summer time 500 hPa geopotential height EOF for analysis (R2) and experiments during summer. The percent variance is indicated by percent in each panel.

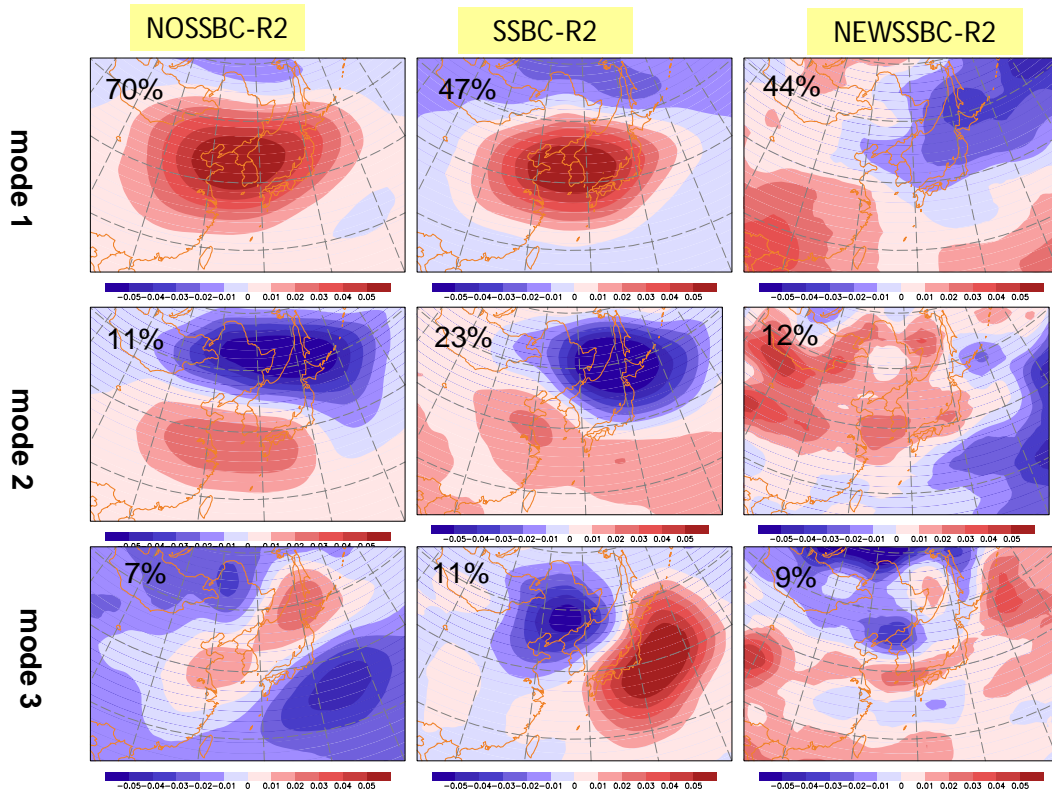


Figure 7. First three modes of the EOF of 500hPa height model error. Percent variances are also indicated in each panel.

500-HGT EOF DJF

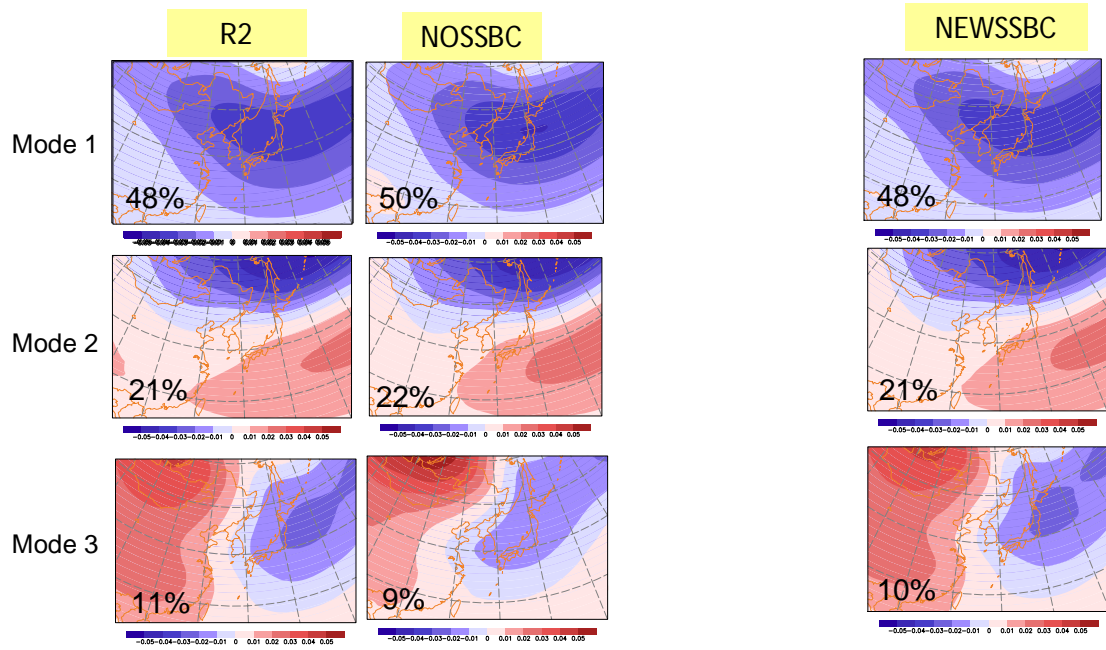


Figure 8. Same as Figure 6, but during winter.

linear trend of 500-hPa height

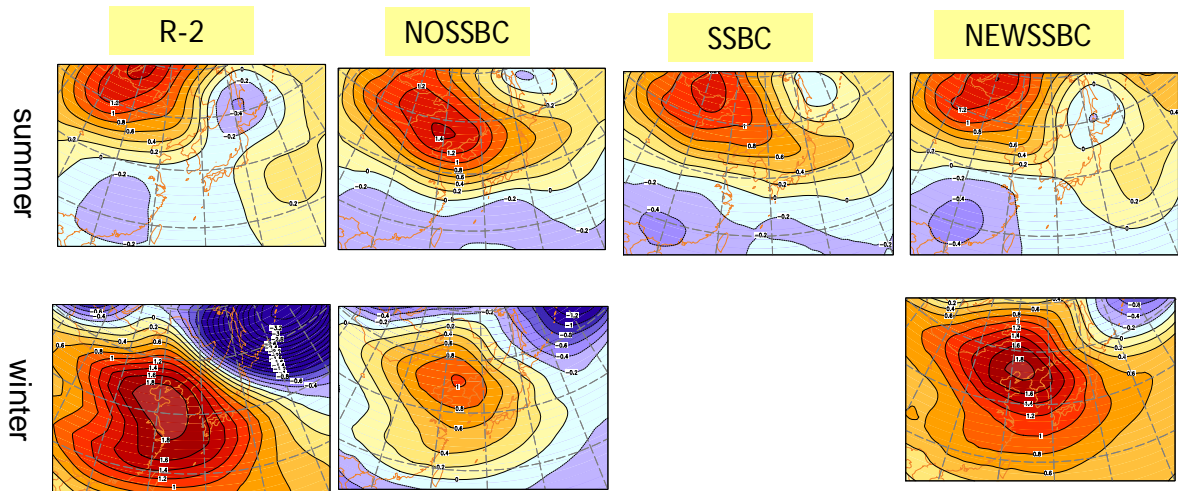


Figure 9. 1972-2005 linear trend of 500 hPa height for summer (upper panels) and winter (lower panels). Unit in meter/10 years.

Precipitation (mm)

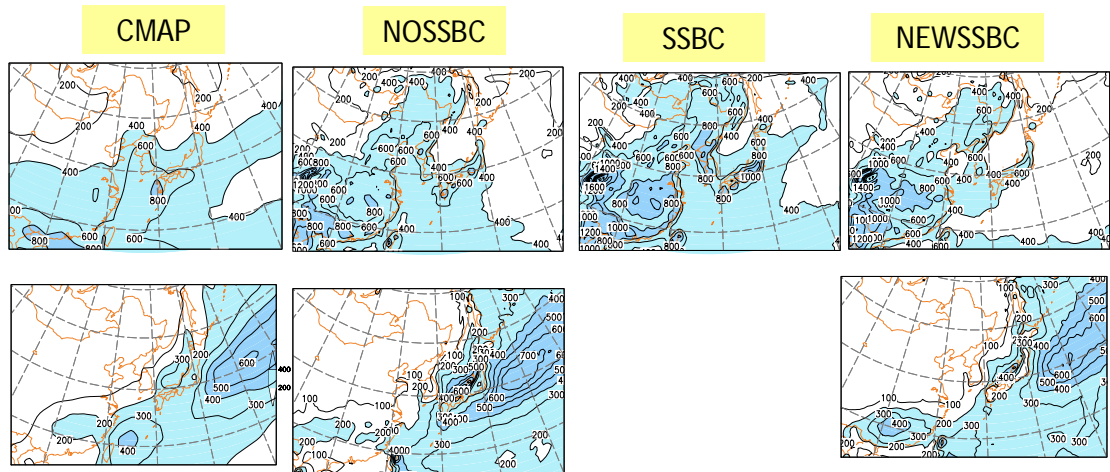


Figure 10. 1978-2005 climatology of precipitation for summer (upper panes) and winter (lower panels). Unit in mm/month.

EOF of Precipitation (summer)

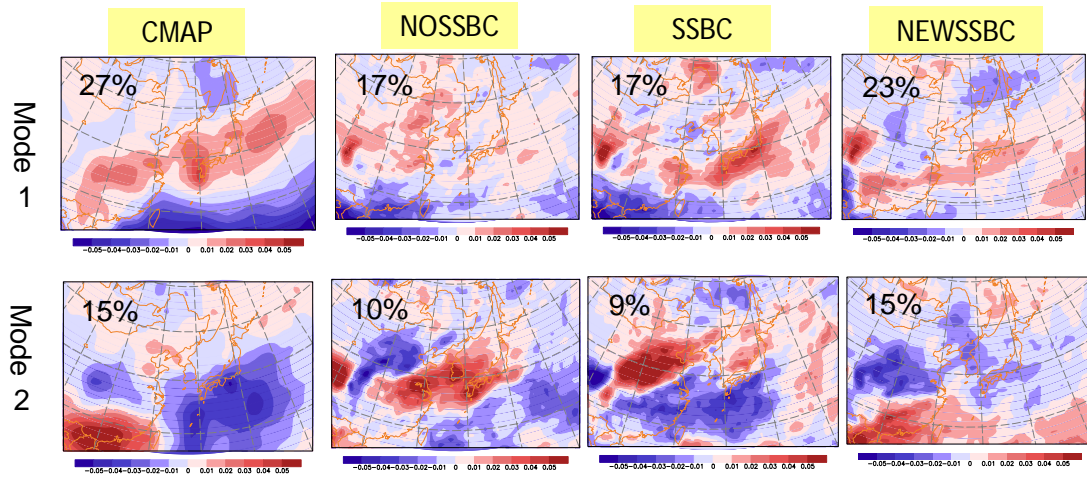


Figure 11. First two leading EOF of seasonal mean precipitation during summer from observation (R-2) and experiments.

EOF Precipitation (winter)

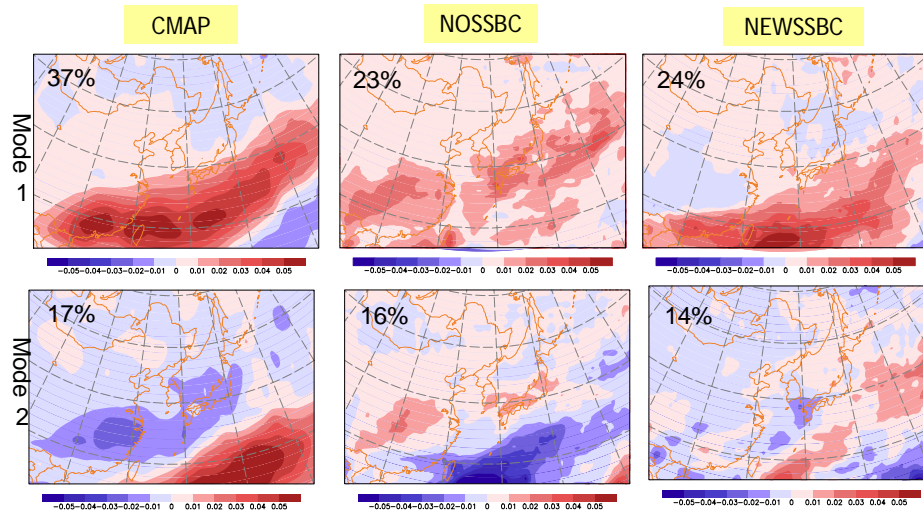


Figure 12. Same as Figure 11 but for winter.

linear trend of precipitation

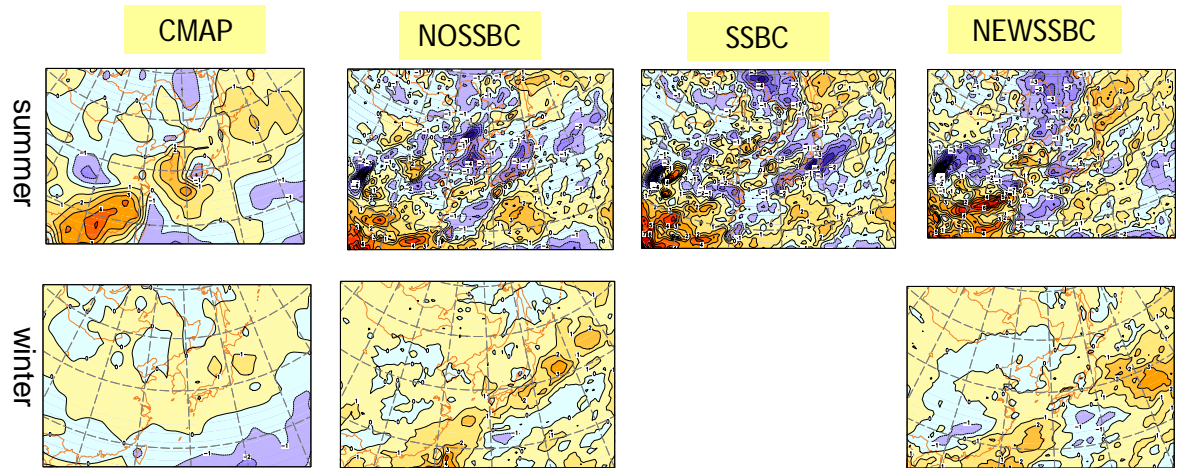


Figure 13. 1978-2005 linear trend of precipitation during summer (upper panels) and winter (lower panels). Unit in mm/10 years.

linear trend of surface temperature (summer)

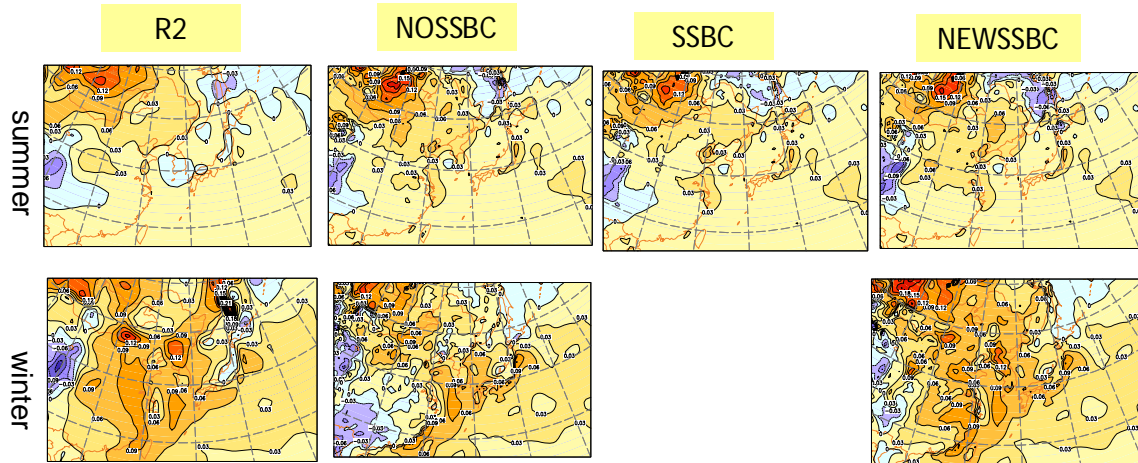


Figure 14. 1978-2005 linear trend of near surface temperature during summer (upper panels) and in winter (lower panels). Unit in mm/10 years.

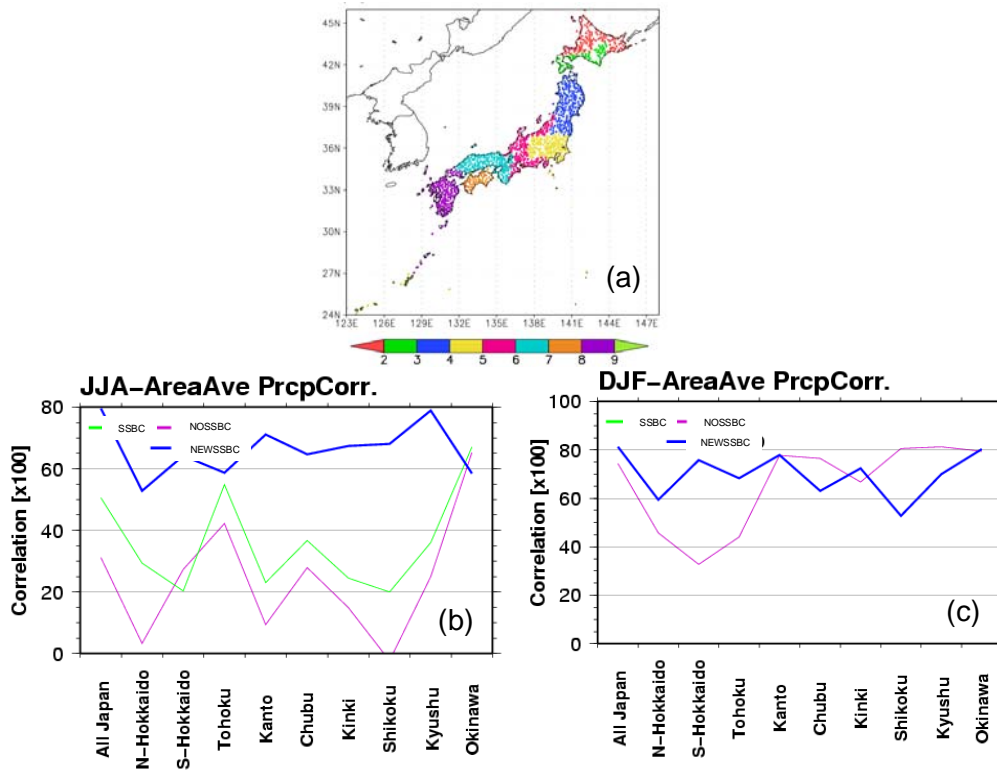


Figure 15. Temporal correlation of precipitation at AMeDAS stations average over sub-domains in summer (b) and winter (c). The domains are color coded (a) by orange (N-Hokkaido), green (S- Hokkaido), magenta (Tohoku), yellow (Kantou), red (Chubu), blue (Kinki), brown (Shikoku), purple (Kyushu) and light green (Okinawa).

References

- Alexandru, A., R. de Elia, and R. Laprise, 2007: Internal Variability in Regional Climate Downscaling at the Seasonal Scale *Mon. Wea. Rev.* 135, 3221–3238 DOI: 10.1175/MWR3456.1
- Gochis, D. J., W. J. Shuttleworth, and Z.-L. Yang (2002), Sensitivity of the modeled north American monsoon regional climate to convective parameterization. *Mon. Weather Rev.*, 130, 1282-1297.
- Hong, S.-Y., and A. Leetmaa (1999), An evaluation of the NCEP RSM for regional climate modeling. *J. Clim.*, 12, 592-609.
- Hong, S.-Y., Y. Noh, and J. Dudhia (2006), A new vertical diffusion package with an explicit treatment of entrainment processes, *Mon. Weather Rev.*, 134, 2318-2341.
- Juang, H.-M. H., S.-Y. Hong, and M. Kanamitsu (1997), The NCEP regional spectral model: An update. *Bull. Am. Meteorol. Soc.*, 78, 2125-2143.
- Juang, H.-M. H., and M. Kanamitsu (1994), The NMC nested regional spectral model, *Mon. Weather Rev.*, 122, 3-26.
- Kanamitsu, M., W. Ebisuzake, J. Woollen, S.-K. Yang, J. J. Hnilo, M. Fiorino, and G. L. Potter (2002), NCEP-DOE AMIP-II Reanalysis (R-2), *Bull. Am. Meteorol. Soc.*, 83, 1631-1643.
- Kang, H.-S., and S.-Y. Hong, 2008: Sensitivity of the simulated east Asian summer monsoon to four convective parameterization in a regional climate model. *J. Geophys. Res.*, 113, D15119, doi:10.1029/2007JD009692.
- Kida, H., T. Koide, H. Sasaki, and M. Chiba, 1991: A New Approach for Coupling a Limited Area Model to a GCM for Regional Climate Simulations. *J. Meteor. Soc. Japan*, 69, 723-728.

- Kusunoki, S., J. Yoshimura, H. Yoshimura, A. Noda, K. Oouchi and R. Mizuta, 2006:
Change in Baiu Rain Band in Global Warming Projection by an Atmospheric
General Circulation Model with a 20-km Grid Size. *J. Met. Soc. Japan.*, **84**,
581-611.
- Mahrt, L., and H.-L. Pan (1984), A two layer model of soil hydrology, *Bound. Layer
Meteor.*, 29, 1-20.
- Reynolds, R. W., and T. M. Smith (1994), Improved global sea surface temperature
analyses using optimum interpolation, *J. Clim.*, 7, 929-948.

